



## **RED SQUIRREL Tests – Air Products Ammonia Field Experiments**

**S. Dharmavaram**

Air Products  
Allentown, PA, USA  
dharmas1@airproducts.com

**M. J. Carroll**

Air Products  
Allentown, PA, USA  
carrolmj@airproducts.com

**E. M. Lutostansky**

Air Products  
Allentown, PA, USA  
lutostem@airproducts.com

**D. McCormack**

Air Products  
Hersham, UK  
mccormd1@airproducts.com

**A. Chester**

DNV  
Spadeadam, UK  
alastair.chester@dnv.com

**D. Allason**

DNV  
Spadeadam, UK  
daniel.allason@dnv.com

Prepared for Presentation at  
American Institute of Chemical Engineers  
2023 Spring Meeting and 19th Global Congress on Process Safety  
Houston, TX  
March 12-16, 2023

AIChE shall not be responsible for statements or opinions contained  
in papers or printed in its publications

# RED SQUIRREL Tests – Air Products Ammonia Field Experiments

S. Dharmavaram<sup>1</sup>, M.J. Carroll<sup>1</sup>, E.M. Lutostansky<sup>1</sup>, D. McCormack<sup>2</sup>, A. Chester<sup>3</sup>, and D. Allason<sup>3</sup>

<sup>1</sup> Air Products, Allentown, PA, USA; <sup>2</sup> Air Products, Hershaw, UK; <sup>3</sup> DNV, Spadeadam, UK

## Abstract

The Red Squirrel ammonia field experiments were conducted at the DNV Spadeadam site in U.K. in 2022. Field test data currently exists for high pressure (ambient temperature) two-phase releases of ammonia from Desert Tortoise (1983) and FLADIS (1996) experiments. No field tests have ever been done for cold (refrigerated) ammonia liquid spills on dry land or into water. The handling of liquified ammonia, during storage/processing and transportation, in a cold (refrigerated) state is inherently safer than in high pressure (ambient temperature) liquified state. The main objective of the Air Products Red Squirrel Tests was to determine the source term and dispersion characteristics for high pressure (ambient temperature) liquified ammonia and low pressure (cold/refrigerated) liquified ammonia in form of two-phase releases and liquid spills, respectively. Liquid spills on concrete and water were studied, along with the process conditions that led to the transition from liquid spills to two-phase flow regimes based on discharge pressures for cold liquified ammonia. Details on the equipment, instrumentation, secondary containment, and ammonia sensors and their layout are presented. An initial analysis of the source terms and dispersion behavior for two-phase releases and contained liquid spills over a range of weather conditions is also provided.

**Keywords:** Red Squirrel, Ammonia, Field Testing, Pressurized Ammonia, Refrigerated Ammonia, Two-Phase Releases, Spills on Land, Spills on Water

## 1 Introduction

Anhydrous ammonia was discovered around 2500 years ago and has been used for centuries in the chemical and fertilizer industries as a pure material (e.g. in agriculture, refrigeration) and for production of nitrogen containing compounds (e.g. amines, ammonium nitrate). It is also used and sold as aqueous ammonia (in concentrations ranging up to 30%) in a variety of other applications like cleaning, food production, etc. Today, ammonia is the second most produced chemical, after sulfuric acid, with a total global production rate of around 180 million tonnes (MT) per year [1]. About 80% of it is used in the fertilizer industry, and 20 MT per year are globally traded.

In the future, the supply and demand for anhydrous ammonia is expected to increase dramatically. Additional applications for ammonia use as a fuel for electricity production, marine transport, and as a hydrogen carrier will lead to global production rates of 500 MT per year or more by 2050 [2]. The greatest increase in demand for Blue (with CO<sub>2</sub> sequestration) and Green (no CO<sub>2</sub> byproduct) ammonia production is being driven by the decarbonization goals established by various countries. Blue and green ammonia will be produced and transported worldwide as a carrier ultimately for production of blue and green hydrogen, from ammonia cracking, at receiving terminals worldwide. With the increase in demand for production and

handling of anhydrous ammonia, there is a need to thoroughly understand the consequences of loss of containment and thus the development of inherently safer designs/processes for production, handling, and transport.

Ammonia vapor is lighter than air, buoyant, and disperses easily, but ammonia liquid compressed under pressure forms a dense plume upon loss of containment. The behavior of ammonia vapor and two-phase plumes are different from chlorine vapor or two-phase plumes that are both heavier than air, while both ammonia and chlorine have a similar boiling point (-33 to -34 °C). The fluid discharge of compressed chlorine and ammonia at ambient temperatures is similar, with formation of fine aerosol and dense plumes. Detailed large-scale field tests have been done for chlorine, called Jack Rabbit II [3], but something similar is needed for anhydrous ammonia to understand the source terms and the near-field and far-field dispersion behavior.

Like chlorine, ammonia is acutely toxic, and exposure to high concentrations results in severe irritation (of eyes, nose, throat, etc.) and respiratory distress. The Emergency Response Planning Guideline (ERPG) concentrations published by the American Industrial Hygienists Association [4] can be used to determine the acute toxicity effects. The ERPG-2 and ERPG-3 concentrations for ammonia are 150 ppm and 1500 ppm, respectively. ERPG-2 is a concentration above which irreversible injuries can occur. Very serious injuries and potential fatalities can occur based on exposure time at concentrations above ERPG-3. The probability of fatality can be determined using Specified Level of Toxicity (SLOT) and Significant Likelihood of Death (SLOD), and Dangerous Toxic Load (DTL) data published by the U.K. Health and Safety Executive (see Table 1) [5]. Chlorine is more toxic than ammonia, and the relative numbers are shown below for comparison.

**Table 1: SLOT and SLOD DTLs for Ammonia and Chlorine [5]**

Substance name	CAS number	'n' value	SLOT DTL (ppm <sup>n</sup> .min)	SLOD DTL (ppm <sup>n</sup> .min)
Anhydrous Ammonia	7664-41-7	2	$3.78 \times 10^8$	$1.03 \times 10^9$
Chlorine	7782-50-5	2	$1.08 \times 10^5$	$4.84 \times 10^5$

Several ammonia incidents have occurred that have resulted in serious injuries and fatalities, and worst among them is the Dakar accident in 1992 [6, 7]. However, very limited information and data exists on the behavior of anhydrous ammonia after a loss of containment. At ambient temperature and atmospheric pressure, ammonia is a gas that is lighter than air. Currently, most of the ammonia is transported on road at ambient temperatures in a pressurized state (as a compressed gas) at pressures of 7 to 10 barg. At these high pressures, the loss of containment results in a 2-phase fluid flow and the ammonia released (typically 88% liquid after flashing, which is in fine aerosol form) is very heavy and dense resulting a plume that travels to long-distances to concentrations of concern mentioned above. The Desert Tortoise field experiments [8] were conducted in 1983 and clearly demonstrated the 2-phase flow and dense fluid behavior of the ammonia when released over time in large-scale tests, as a warm liquid under pressure. An additional series of small-scale tests [9] were conducted in Sweden in 1996 (called FLADIS tests) that confirmed the behavior of liquified ammonia at ambient temperature and high pressures.

Refrigerated or cold ammonia (at low temperatures [ $<-30$  C] and low pressures [ $< 1$  barg]) is expected to be inherently safer to store, handle, and transport. All the liquid ammonia transported from production facilities to receiving terminals is handled in ships and barges in a cold/refrigerated state. The cold liquid ammonia at the terminals is stored in large flat-bottomed

tanks at low pressures. Loss of containment of low pressure, cold ammonia results in a smaller discharge rate (compared to two-phase discharges for high pressure releases) and a liquid spill that would eventually boil off from any surface it is spilled on. The vapors resulting from the boiling phenomenon are warmer and expected to be buoyant because of the low vapor density compared to ambient air. The buoyant plume can then disperse easily with limited downwind impacts at ground level. However, no data currently exists on the behavior of liquid spills on land or onto (or under) water. The behavior of cold ammonia accidentally released at low to high pumping pressures for example from pipelines is also not well understood.

The primary purpose of this paper is to share information on the Air Products – Red Squirrel field tests for small-scale liquid ammonia releases conducted at the DNV Spadeadam site in the U.K, in 2022. Also included is an initial analysis of the discharge (source terms) and observed dispersion behavior for the different tests.

## **2 Red Squirrel Tests**

Red squirrels are a native species limited currently to small sections of Northern England and Scotland in the U.K. The name Red Squirrel was chosen for the Air Products tests, since the actual release tests were conducted in Northern England at the Det Norske Veritas (DNV) Spadeadam site. Red Squirrel tests and data thus generated will be used to drive decisions for inherently safer design and operations for handling liquid ammonia at facilities worldwide.

It is important for Air Products and the industry to demonstrate that storing, handling, and transporting liquid ammonia at production and receiving terminals in a cold/refrigerated state (even on road & rail, in addition to marine transport) is inherently safer than at ambient temperature (and high pressure) and is a better practice for the long-term when the supply and demand in the next few years is dramatically more than the current situation in 2023.

### ***2.1 DNV Spadeadam Site***

The DNV research and testing site in Spadeadam, U.K., has been conducting major hazards research since the 1970s, see Figure 1. Detailed field testing has been conducted to understand major accident hazards, leading to better understanding of consequences of accidents following significant incidents like Piper Alpha, Flixborough, Buncefield, etc. By conducting tests under controlled conditions, data and findings have been generated to help government agencies, industrial partners, and others drive decisions to ensure safe designs & operations. A major focus of the research and testing has been on fires and explosions for a variety of flammable chemicals and explosive substances. More recently, testing has been expanded to address the consequences of loss of containment of cryogenics/asphyxiants (e.g. liquid N<sub>2</sub>, liquid natural gas, liquid hydrogen, supercritical CO<sub>2</sub>) and acute toxins (e.g. liquid NH<sub>3</sub>).

The weather conditions at the Spadeadam site are quite variable and unpredictable. For conducting the Red Squirrel tests, appropriate dates and times were selected, while ensuring that there was no precipitation and wind speeds were above the minimum to avoid off-site impacts. It took almost the entire 2022 to conduct the tests described below.



Figure 1: DNV Spadeadam Site

## 2.2 Red Squirrel (RS) Tests – Equipment, Instrumentation, & Measurements

The test setup for the RS tests is shown in Figure 2 below. The refrigerated, unpressurized releases for RS-1 were done using the ammonia release vessel at the bottom of the figure as well as the ammonia discharge vessel and release orifice at the top to increase the amount of ammonia released over a short time into a bund. With this, the release vessel could provide a large release rate for a short time whilst the discharge vessel provides a lower release rate over a longer duration. Both the refrigerated and ambient temperature pressurized releases (RS-2 and RS-3) utilized the ammonia discharge vessel and release orifice shown at the top of the Figure 2.

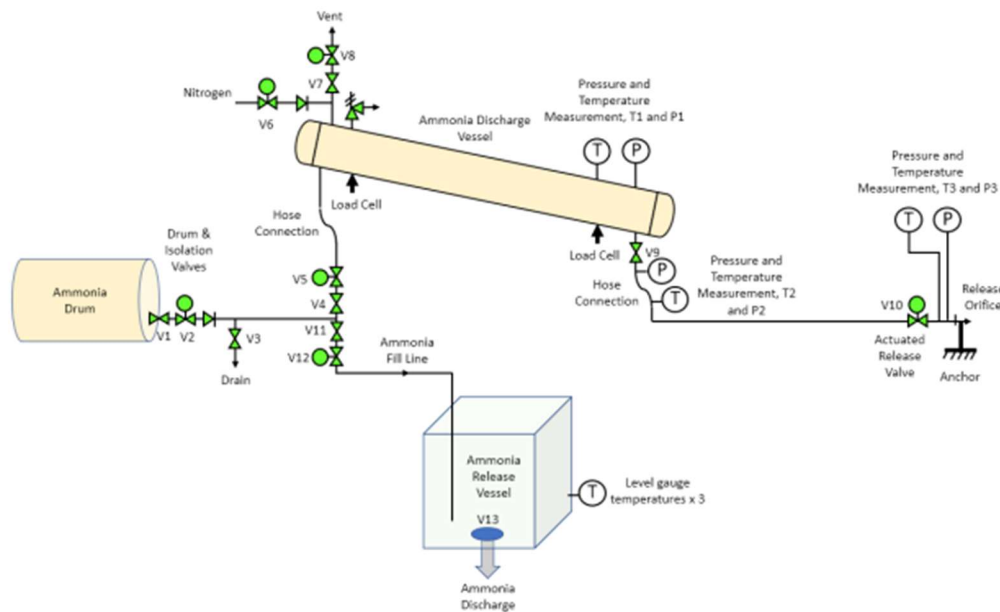
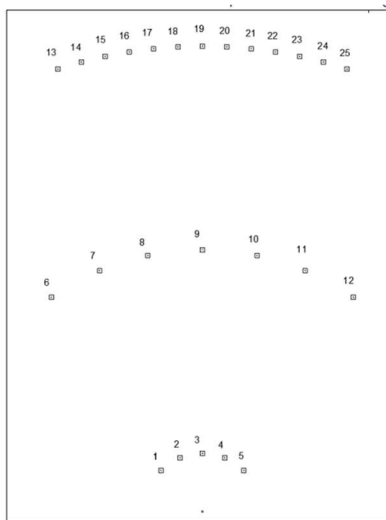


Figure 2: Equipment discharge configuration for the Red Squirrel tests

Several instruments were installed during the RS tests to get data for crucial parameters for different types of liquid ammonia releases (further described below). All the instruments were operated using manufacturer's calibration data or field calibration as appropriate. There was some variability in type of instrumentation and their locations based on the tests, from the following list:

- Ammonia concentration monitors in field with co-located thermocouples
- Vessel, piping, and orifice temperature and pressure sensors
- Wind speed, wind direction, relative humidity, ambient temperature, ambient pressure
- Normal speed videos (stationary cameras)
- Unmanned Aerial Vehicle (UAV) visual footage
- Thermal imaging
- Mass sensors for ammonia in vessel and bund
- Thermocouples on the bund concrete surface temperatures and in the air above bund
- Bund water pH sensors

The positions of the ammonia concentration monitors in the field are shown in Figure 3 below. Note that this setup was used for all trials except RS-2A to RS-2D. All sensors at 10 m and 45 m were at a height of 2 m, however, sensors at 80 m varied from 2 m, 6 m, to 10 m in height. The sensors were laid out in the expected wind direction plus maximum angles of 45°, 36°, and 18°, respectively, at each distance to capture the centerline concentrations. Note that all sensors had a maximum reading of about 1100 ppm. Data from these sensors was used to evaluate dispersion modeling performed using weather measurements along with source terms created from other instrument data such as temperature, pressure, and mass.



**Figure 3: Location of Ammonia Sensors at 10 m, 45 m, and 80 m arcs from release point**

For the spills onto concrete, thermocouples on the base of the bund captured the temperature decrease that occurred during the pool vaporization. The layout of these is shown below in Figure 4. For spills into water, pH sensors on the bund base measured the pH of the water at various locations, shown in Figure 5 below.

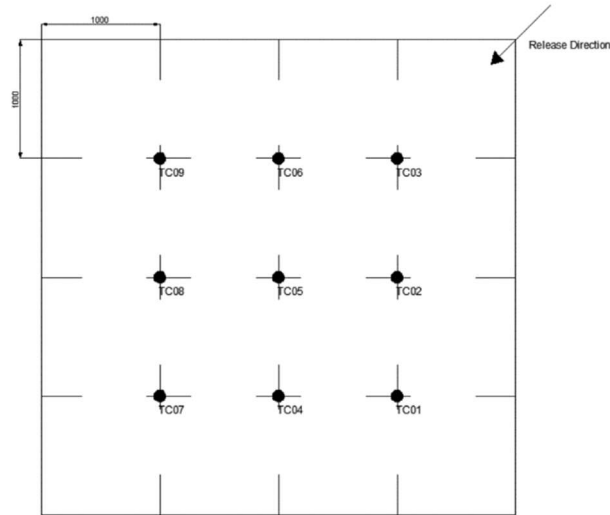


Figure 4: Location of thermocouples in base of the bund for RS-1C and RS-1D

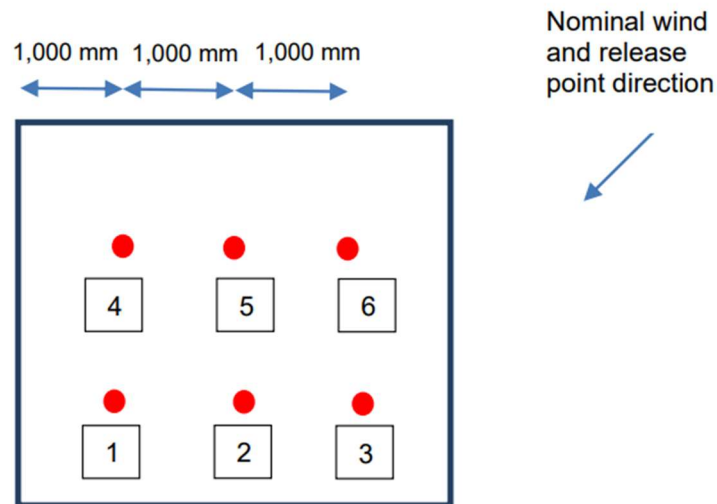
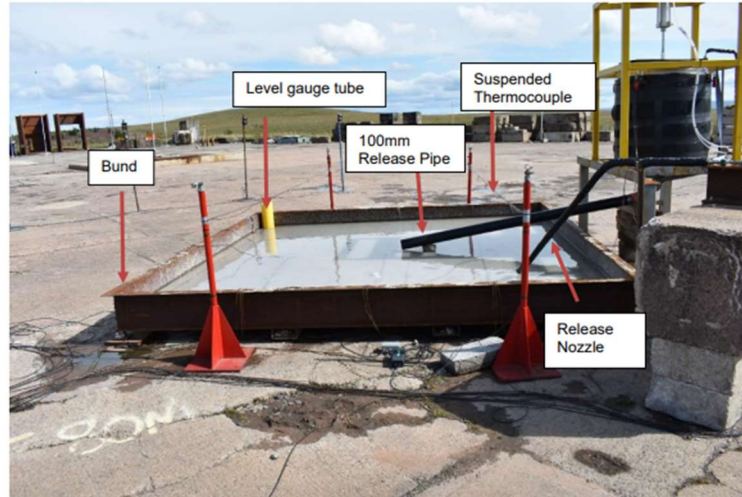


Figure 5: Location of pH sensors in base of the bund for RS-1F and RS-1G

## 2.3 Red Squirrel – 1 (RS-1), Red Squirrel – 2 (RS-2), and Red Squirrel – 3 (RS-3) Tests

### 2.3.1 RS-1 (Refrigerated/Cold, Unpressurized Ammonia on Concrete and Water)

The RS-1 tests were performed with refrigerated/cold unpressurized ammonia released quickly into a 4 m x 4 m x 0.3 m bund with a concrete base (see Figure 6) from two separate vessels (see Figure 2). For the RS-1C and RS-1D tests ammonia was released into an empty bund over a short duration (20 seconds) through the release pipe and release nozzle from the two vessels. For the RS-1F and RS-1G tests a small amount of ammonia was released from just the discharge vessel the surface into the bund filled with 1000 L water.



**Figure 6: Unpressurized cold ammonia spills into a bund on concrete or water**

A summary of the RS-1 tests and conditions are provided in Table 2. Side views of the RS-1C and RS-1F release plumes are shown in Figures 7 and 8, respectively.

**Table 2: RS-1 Tests Summary**

Tests	Bund Surface Type	Liquid Released (kg)	Release Duration (s)
RS-1C	concrete	344	358
RS-1D	concrete	291	367
RS-1F	water	136	18
RS-1G	water	136	22



**Figure 7: RS-1C unpressurized/cold ammonia spill on concrete in bund**





**Figure 8: RS-1F unpressurized/cold ammonia spill on water in bund with initial puff discharge for 18 seconds (left) and aqua ammonia pool after release (right)**

2.3.2 RS-2 (Ambient Temperature, Pressurized Ammonia Releases)

The RS-2 tests were performed with ambient temperature, pressurized ammonia. All the tests were performed as horizontal releases through a 6 mm orifice elevated 1 m from the ground from the ammonia discharge vessel shown in Figure 2. A summary of the RS-2 tests and conditions are provided in Table 3. A side view of the RS-2F two-phase plume is shown in Figure 9.

**Table 3: RS-2 Tests Summary**

Tests	Release Pressure (barg)	Release Temperature (C)	Amount Released (kg)	Discharge Duration (s)
RS-2A	3	0	109	839
RS-2B	8.5	0	95	169
RS-2C	9	-2	84	160
RS-2D	6	1.5	92	300
RS-2E	3.25	0	154	704
RS-2F	3.75	0	197	1473



**Figure 9: RS-2F pressurized ambient temperature ammonia release**

2.3.3 RS-3 (Refrigerated, Pressurized Releases)

The RS-3 tests were done with refrigerated/cold ammonia, released under pressure imposed by nitrogen. For these tests, the releases were directed downward at a 45° angle through a 6 mm orifice, into a concrete bund to increase the likelihood of capturing all liquid in the bund area. At low pressures, much of the liquid discharged is in fact collected in the bund. At high pressures, the fluid is deflected from the surface of the concrete with small amounts of liquid collected in the bund. A summary of the RS-3 tests and conditions are provided in Table 4. Side views of the RS-3A and RS-3F releases & plumes are shown in Figure 10 and Figure 11 below.

**Table 4: RS-3 Tests Summary**

Tests	Release Pressure (barg)	Vessel Temperature (C)	Liquid Released (kg)	Discharge Duration (s)
RS-3A	0.3	-30	133	1951.5
RS-3B	0.33	-28	132	2305.5
RS-3C	1	-29	103	270
RS-3D	2	-28	152	193
RS-3E	4	-30	65	100
RS-3F	5	-29	148	160



**Figure 10: RS-3A refrigerated, pressurized ammonia release**



**Figure 11: RS-3F refrigerated, pressurized ammonia release**

### 3 Results

Vaporization and dispersion modeling was done when applicable for each of the trials using PHAST Version 8.23 [10]. The experimental data was used to generate vaporization rates, release rates, and other source term components. Data on wind speed and direction and temperature were used to create weather scenarios for each trial. For all daytime trials, D was assumed for Pasquill stability with F for night. Due to the large variability in wind speed and direction, dispersion models were run with the average wind speed for the period of interest as well as plus and minus one standard deviation in the wind speed. To find centerline concentrations, ammonia monitors with highest readings were used and moving averages of about 60 seconds were applied (with 30 seconds applied for short releases). These averaging periods were then used as the averaging times for the dispersion modeling in PHAST.

### 3.1 Cold Ammonia Spills on Dry Concrete (RS-1)

For the RS-1 refrigerated, unpressurized ammonia releases onto concrete, liquid ammonia was released for approximately one minute into the concrete bund, and then the bund mass and field concentrations were monitored for a number of hours. First, the trials were analyzed over the first half-hour post release with the pool vaporization.

Experimental data as well as PHAST pool vaporization model results for the first half-hour post release is shown in Table 5. Here, the start mass represents the amount of ammonia in the bund right as the release stopped and the end mass is the amount remaining after 30 minutes of vaporization. The experimental vaporization rate was determined by taking the difference between these values and dividing by vaporization time. The rate in PHAST was determined by setting up a pool vaporization with the experimental start mass, a temperature of  $-34^{\circ}\text{C}$ , and the experimental wind speed, ambient temperature, and relative humidity. Additionally, a solar radiation flux of  $100 \text{ W/m}^2$  was assumed for both trials. Both trials show good agreement between the experimental data and rate and the PHAST model results, although PHAST does slightly overpredict how much ammonia boils off. As seen in Figure 12, the PHAST model resulted in a higher vaporization rate at the beginning which then flattened out as the concrete cooled, which might explain the low final mass of ammonia. It all depends on how models account for ground effects, and mass & heat transfer resistance. In reality, the vaporization rate for a fixed pool area should be at a fairly flat rate as shown by the RS-1C data (shown in Figure 12) collected and as previously discussed by Studer et al. [11].

**Table 5: Mass and vaporization rate values for the 1<sup>st</sup> 30 minutes post release for concrete spills**

Variable	RS-1C	RS-1D
experimental start mass (kg)	249	257
experimental end mass (kg)	138	161
experimental rate (kg/s)	0.061	0.053
PHAST start mass (kg)	249	257
PHAST end mass (kg)	107	154
PHAST rate (kg/s)	0.05 – 0.08	0.035 – 0.06

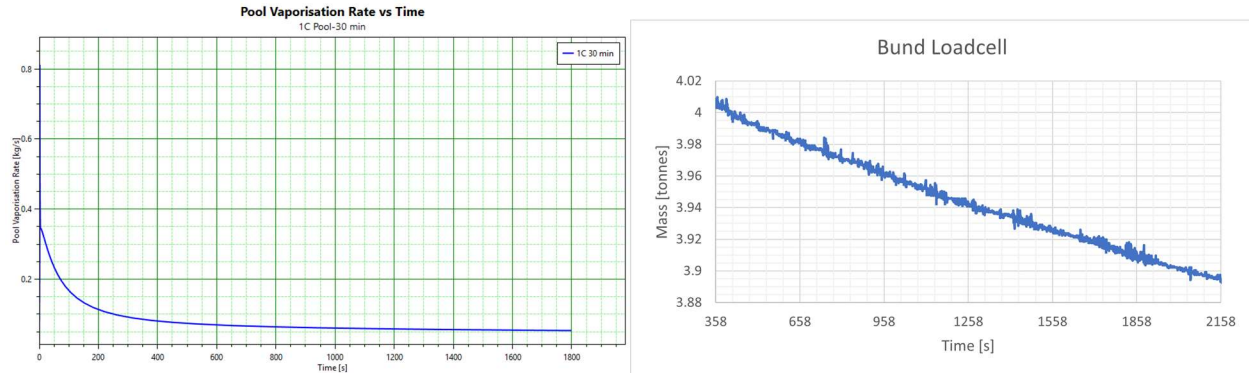


**Figure 12: PHAST vaporization rate model (left) compared to experimental mass vs time data (right) for RS-1C during the 1<sup>st</sup> 30 minutes post release**

In addition to the vaporization rates, the temperatures of the ammonia pool were analyzed both during the release (up until about 360 seconds) and for the hour after. Figure 13 below shows the readings from the thermocouples in the base of the bund during this time for trial RS-1C. Almost instantly, the temperature readings go from the ambient temperature of 18°C to about -34°C, the temperature of the refrigerated ammonia. However, once the release finishes and vaporization begins to occur, instead of the ammonia temperature increasing due to contact with the atmosphere, it actually decreases to about -60°C at the concrete surface. Due to the heat and mass transfer mechanisms of ammonia boil-off [11], this was an anticipated result. As the concentration of the vapor above the pool drops below 100% ammonia due to wind dilution, the temperature in the pool decreases. These observations can inform design decisions about design temperatures for ammonia containing equipment, where rapid vaporization is a concern. Note that some sensor readings begin to increase back to atmospheric temperature as boil-off continues. This may indicate that certain areas of the bund dry up as the pool recedes.

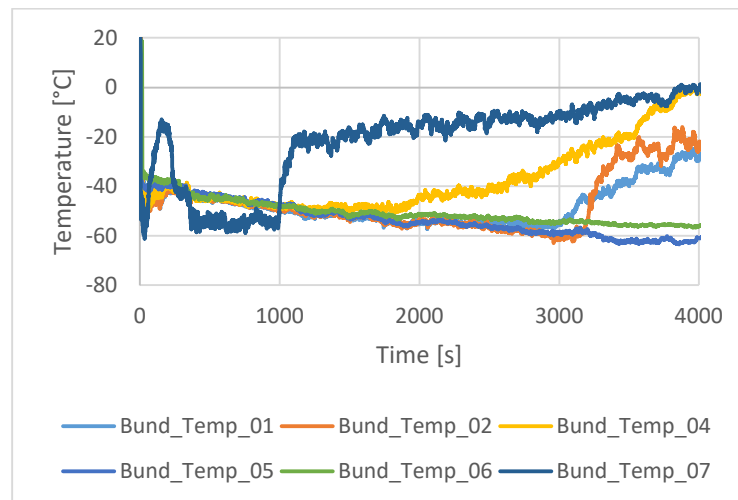


**Figure 13: Temperature data from thermocouples in bund base during release and vaporization for RS-1C**

The experimental data for the field concentrations are shown in Table 6 below for trials RS-1C and RS-1D. Data is shown both for the first hour and second hour post release to show how long the dispersed ammonia remains in the effect zone.

The concentration data for the first hour shows that while the concentration is quite high in the near field, it is not so high in the far field when compared to two-phase horizontal releases discussed below. This is likely because ammonia is boiling off mostly in the vertical direction and only travels into the field due to the wind bending the centerline, and not the initial momentum from a release. A comparison between the first- and second-hour post release shows a significant decrease in concentration due to lower vaporization rates. At 45 m and beyond, the ammonia is below ERPG-2 levels.

**Table 6: Experimental concentrations (ppm) for RS-1C and RS-1D for the 1<sup>st</sup> and 2<sup>nd</sup> hours post release**

Sensor	RS-1C		RS-1D	
	1 <sup>st</sup> Hour Post	2 <sup>nd</sup> Hour Post	1 <sup>st</sup> Hour Post	2 <sup>nd</sup> Hour Post
10 m	>1100	300-425	>1100	500-700
45 m	100-220	20-40	200-300	45-100
80 m, 2 m	50-100	7-13	125-175	18-60
80 m, 10 m	30-80	0	40-60	6-13

PHAST was used to model the dispersion of the ammonia vaporizing from the pool for the first hour post release and the predicted values were compared to experimental concentration data. To do so, user defined sources were created and used in conjunction with custom weathers. The source terms were vertical leaks with an elevation of 0.3 m. They were modeled as vapors with a temperature just above the boiling point of ammonia and velocities of 0.01 m/s. Experimental vaporization rates for the first hour post release was determined from the bund mass data and used as mass flow rates in the source term. The resulting input parameters and weather data used are shown in Table 7 below.

**Table 7: Inputs for the weather condition and user defined source term to model dispersion for 1<sup>st</sup> hour post release in PHAST**

PHAST Input	RS-1C	RS-1D
wind speed (m/s)	7.5 ± 1.8	3.5 ± 1.0
ambient temperature (C)	18.0	18.7
release phase	vapor	vapor
mass flow (kg/s)	0.047	0.043
velocity (m/s)	0.01	0.01
final temperature (C)	-33	-33

The side view of the dispersion model result for RS-1C is shown in Figure 14 below. The three concentration values shown are for ERPG-2, ERPG-3, and the estimated visible cloud concentration, respectively. The visible cloud concentration was estimated from dew point calculations using experimental atmospheric and ammonia data.

In the model, the estimated visible cloud concentration of 11800 ppm (based on dewpoint) extends to a maximum distance of 4 m which agrees well with the visible cloud seen in Figure 7. Despite the vertical release, the cloud does not rise above 5 meters and mostly stays along the ground as the wind bends the plume centerline and disperses it, as expected. It is worth noting that the PHAST model predicts the ERPG-2 level extends 72 m away and the ERPG-3 level extends 20 m away from the orifice.

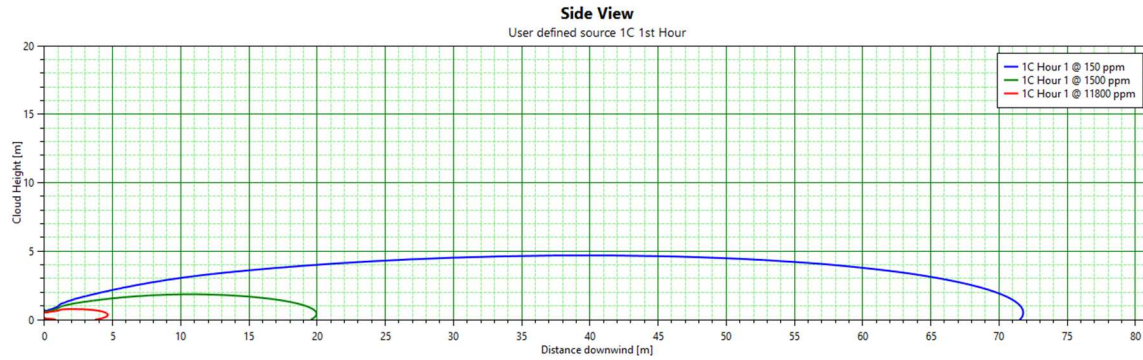


Figure 14: Side view of the PHAST dispersion model for RS-1C for the 1<sup>st</sup> hour post release

Figure 15 below shows concentration vs distance plots for the PHAST model predictions and experimental concentration data for RS-1C and RS-1D. Note that experimental data represented by green dots are values where the sensors were maxed out at 1100 ppm. The plots show that the PHAST dispersion models do in fact predict concentrations >1100 ppm in the near field. The far field values are slightly overestimated by PHAST. However, for both trials at 45 m, the predictions are within a factor of 2 from the experimental results and at 80 m the experimental range overlaps with the predicted range. This is good agreement especially considering the assumptions made about vaporization rate and weather stability and the variation in wind speed and direction. Overall, both the vaporization and dispersion components of spills onto concrete seem to be well characterized by PHAST.

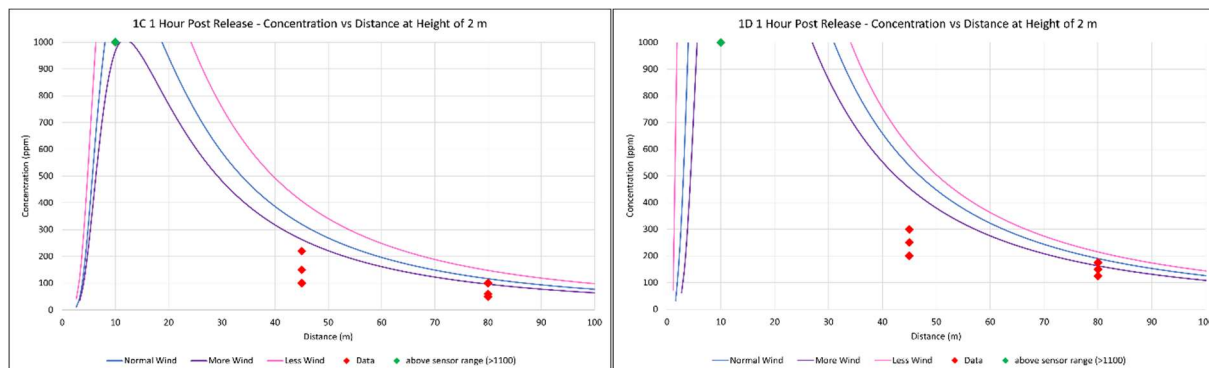


Figure 15: Concentration vs distance experimental data and PHAST model prediction for RS-1C (left) and RS-1D (right) for 1 hour post release

### 3.2 Cold Ammonia Spills on Water in Bund (RS1)

For the RS-1 refrigerated, unpressurized ammonia releases onto water, liquid ammonia was released for approximately 20 seconds into the water-filled concrete bund, and then the bund mass, water pH, and field concentrations were monitored for several hours. First, the trials were analyzed during the duration of the release itself, where some of the ammonia initially deflects off the water surface and continues moving downwind as a puff. Remaining amount of ammonia (approximately 50%) of the total amount spilled is absorbed in the water. Next, the dispersion of the vaporizing ammonia from the aqua ammonia pool during the first hour post release was analyzed.

The experimental data for the field concentrations are shown in Table 8 below for trials RS-1F and RS-1G. Data is shown both for puff duration and the first- and second-hour post release. Note that there seemed to be a miscalibration of the 80 m sensors for RS-1G.

The concentration data for the puff shows very high concentrations in the near field and far field. Although it cannot be determined if the concentrations are greater than the ERPG-3 value of 1500 ppm, this likely indicates a puff from a spill onto water which results in high concentrations but for a short duration at distances downwind. The data for the first-hour post release shows much lower values. Furthermore, the peak values in the concentration ranges occur in the first few minutes after the release, and then the concentrations quickly drop to the lower end of the ranges. This trend was not seen for the concrete releases, indicating that there is a small period of high concentrations when ammonia is spilled into water. This is because unlike with concrete, water absorbs a good fraction (~50%) of the ammonia.

**Table 8: Experimental concentrations (ppm) for RS-1F and RS-1G for the puff and the 1<sup>st</sup> hour post release**

Sensor	RS-1F		RS-1G	
	During Puff	1 <sup>st</sup> Hour Post	During Puff	1 <sup>st</sup> Hour Post
10 m	>1100	200-1000	>1100	200-900
45 m	>1100	25-250	>1100	5-180
80 m, 2 m	>1100	5-100	3	1-2
80 m, 10 m	500-900	2-40	2	1.5

PHAST was used to model the dispersion of the ammonia puff and predicted values were compared to experimental concentration data. To do so, user defined sources were created and used in conjunction with custom weathers. The source terms were vertical leaks with an elevation of 0.3 m. They were modeled as vapors with a temperature just above the boiling point of ammonia and velocities of 0.01 m/s. To determine the mass flow rate, the initial puff mass and release time were needed. To find the puff mass, the mass of ammonia in the bund at the end of the release was subtracted from the total ammonia released, thus assuming all ammonia not absorbed into the water deflected as a puff. It was then assumed that the release rate was constant, so it was determined by dividing the puff mass by release time. The resulting input parameters and weather data used are shown in Table 9 below.

**Table 9: Inputs for the weather condition and user defined source term to model the puff in PHAST**

PHAST Input	RS-1F	RS-1G
wind speed (m/s)	4.8 ± 1.7	5.8 ± 2.4
ambient temperature (C)	8.5	13.0
release phase	vapor	vapor
initial puff mass (kg)	61	58
release time (s)	18	22
mass flow (kg/s)	3.38889	2.63636
velocity (m/s)	0.01	0.01
final temperature (C)	-33	-33

Figure 16 below shows concentration vs time plots for the PHAST model predictions and experimental concentration data for RS-1F for different sensors in the far field. Note that experimental data that plateaus at about 1100 ppm represents a maxed-out sensor. For the 45 m sensor, PHAST does in fact predict values greater than 1100 ppm. However, due to the limitations on the sensor measurements, no more can be determined about the accuracy of the

predictions. The duration of the high concentration readings is about the same for both the model and the data, however the ammonia reaches the sensor much earlier in the PHAST model than in the data. For the 80 m, 10 m high sensor, the PHAST model predicts much higher concentration values over a longer, more sustained duration than what the data shows. Again, the ammonia puff reaches the sensor earlier in the model than in the data.

A possible explanation for the discrepancies in the magnitude of concentrations and travel time to sensor is the high variability in the wind speed and particularly direction during the release. The predictions in Figure 16 only show the differences in wind speed out to one standard deviation, but not the wind direction. While wind speed affects both concentration and the time it takes the puff to reach the sensors, high variability in wind direction would cause the experimental concentrations to decrease.

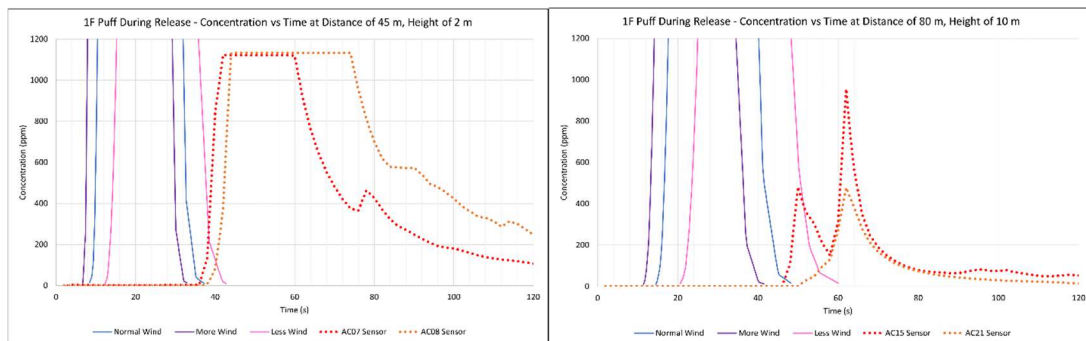


**Figure 16: Concentration vs time experimental data and PHAST model prediction for RS-1F at the 45 m sensor (left) and 80 m, 10 m height sensors (right) for the puff model during the release**

The peak concentrations predicted by PHAST at the 80 m, 10 m high sensors were about 5000 ppm, an order of magnitude larger than the data shows. To determine how the model could be improved, the dispersion parameters were manipulated – particularly the passive near field entrainment parameter. The default value for this parameter of 1 represents the full effect of near field entrainment while a value of 0 represents no near-field passive entrainment. When this parameter was changed to 0, the concentration vs time plot for the 80 m, 10 m sensor was as shown below in Figure 17. Here, the prediction for the less windy condition is about 1000 ppm for the sensor, which is within a factor of 2 of the experimental data. It is possible that further manipulation of other dispersion parameters and weather would improve the model predictions. However, more information from the sensors would be needed to match the near field values.

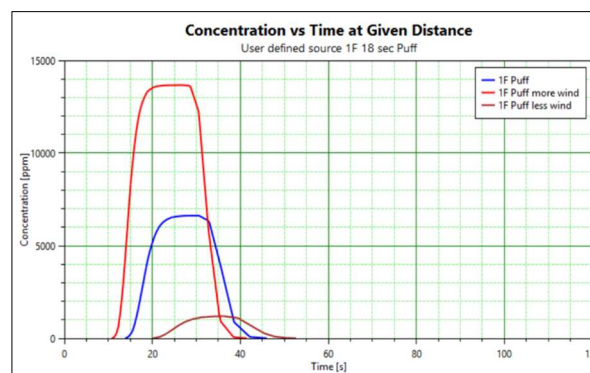


**Figure 17: PHAST model prediction for RS-1F at the 80 m, 10 m height sensor for the puff model during the release**



The experimental data for the first hour post release was analyzed to determine concentrations and pH in the aqua ammonia pool and the vaporization rates for ammonia. The results are shown in Table 10 below. Note that the start mass refers to the mass of ammonia in the pool at the start of the hour, meaning the amount at the end of the release period, and the end mass refers to the mass at the end of the hour. Also note that the initial water seemed to be slightly basic.

For both cases, slightly more than half of the ammonia released ended up dissolved in the water pool. This resulted in a pH of about 11 and an aqua ammonia concentration of about 7% on a mass basis. After one hour of vaporization, the concentration had decreased by 1-1.5% and the pH had decreased slightly. This would show a rather slow vaporization of ammonia from the aqua ammonia pool. To find the vaporization rate, the slope of the ammonia mass versus time plot was found.

**Table 10: Mass, concentration, vaporization rate, and pH data of the aqua ammonia pools in RS-1F and RS-1G for the 1<sup>st</sup> hour post release**

Variable	RS-1F	RS-1G
initial water in bund (kg)	1000	1000
initial water pH	8.5	8.0
total ammonia released (kg)	136	136
experimental start mass (kg)	75	78
percent dissolved (mass %)	55.1	57.3
start concentration (mass %)	7.0	7.2
experimental start pH	11	10.5
experimental end mass (kg)	63	58
end concentration (mass %)	6.0	5.5
experimental end pH	10.75	10.5
experimental rate (kg/s)	0.0033	0.0056

PHAST was used to model the dispersion of the ammonia vaporizing from the pool for the first hour post release and the predicted values were compared to experimental concentration data. To do so, user defined sources were created and used in conjunction with custom weathers. The source terms were vertical leaks with an elevation of 0.3 m. They were conservatively modeled as pure ammonia vapors with velocities of 0.01 m/s. As the ammonia vapor would be mixed with water vapor from the pool, it was assumed to be at ambient temperature. The resulting input parameters and weather data used are shown in Table 11 below.

**Table 11: Inputs for the weather condition and user defined source term to model dispersion for 1<sup>st</sup> hour post release in PHAST**

PHAST Input	RS-1F	RS-1G
wind speed (m/s)	4.7 ± 1.7	8.0 ± 3.5
ambient temperature (C)	8.5	13.0
release phase	vapor	Vapor
mass flow (kg/s)	0.0033	0.0056
velocity (m/s)	0.01	0.01
final temperature (C)	8.5	13

Figure 18 below shows concentration vs distance plots for the PHAST model predictions and experimental concentration data for RS-1F and RS-1G. As noted for Table 8, the high experimental concentration values were from the tail end of the puff and are not representative of

the majority of the first hour post release. The plots show the PHAST dispersion model does a good job predicting concentrations in the near and far field for the data points that are after the tail end of the puff has passed.

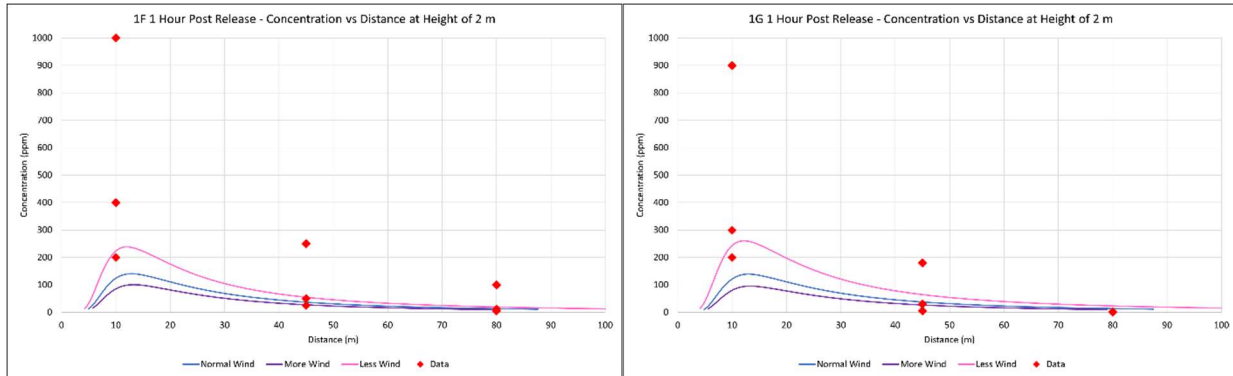


**Figure 18: Concentration vs distance experimental data and PHAST model prediction for RS-1F (left) and RS-1G (right) for 1 hour post release**

### 3.3 Ambient Temperature, Pressurized Ammonia Releases (RS-2)

The RS-2 ambient temperature, pressurized ammonia releases were analyzed for the period during the release itself. The experimental data for the field concentrations are shown in Table 12 below for trials 2D-2F as trials 2A-2C produced poor experimental data. Additionally, the temperature data for 10 m from the release point for RS-2F is shown in Figure 20.

The concentration data shows that even in the far field, the concentration of ammonia is still quite high during the release itself. Particularly for RS-2D, where the release pressure was 6 barg, the sensors at 75 m away from the release are maxed-out, indicating a very large footprint of high concentrations.

The ammonia was released as a two-phase fluid from the orifice at 0 °C for trial RS-2F. As ammonia transitions from a two-phase fluid to a vapor during the discharge phase, it typically drops in temperature and becomes a rather dense vapor. Figure 19 shows that 10 m away from the orifice, the temperature of the ammonia is about -5°C during the release. It is likely that the ammonia became even colder during the expansion zone and then warmed up from the surrounding air as it dispersed from the orifice. This is supported by the temperature data.

**Table 12: Experimental concentrations (ppm) for RS-2 tests for during the release itself**

Sensor	RS-2D		Sensor	RS-2E	RS-2F
25 m	>1100		10 m	>1100	>1100
50 m	>1100		45 m	200-800	200-400
75 m, 2 m	>1100		80 m, 2 m	150-300	100-200
100 m, 2 m	250-350		80 m, 10 m	350-800	200-600
125 m, 2 m	125-300				

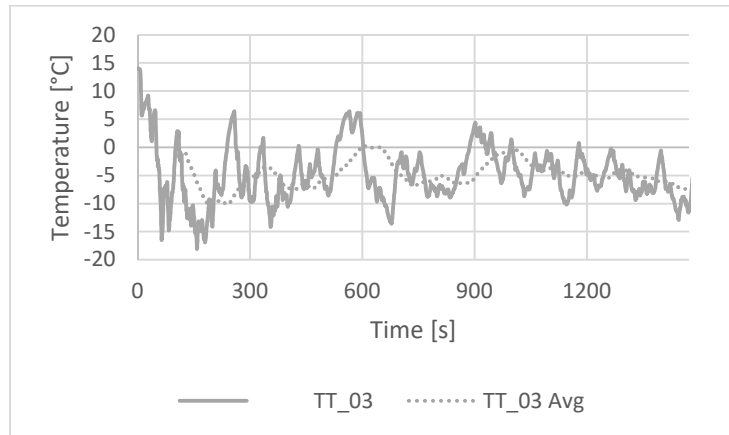


**Figure 19: Temperature data from the thermocouple attached to the centerline 10 m field sensor**

PHAST was used to model the two-phase release of ammonia for the tests and the predicted values were compared to experimental concentration data. Pressure vessels with leaks were used to create user defined sources used in conjunction with custom weathers. The leaks were horizontal and at an elevation of 1 m. The orifice diameter of the leak was set to 6 mm – as it was in the experimental setup – and a user defined source term was developed to match the experimental release rate. The resulting input parameters and weather data used are shown in Table 13 below.

**Table 13: Inputs for the weather condition, pressure vessel, and user defined source term to model dispersion during the release in PHAST**

PHAST Input	RS-2D	RS-2E	RS-2F
wind speed (m/s)	$8.1 \pm 2.7$	$5.0 \pm 1.0$	$4.2 \pm 1.1$
ambient temperature (C)	6.2	1.8	13.6
release temperature (C)	1.5	0	0
release pressure (barg)	6.0	3.5	3.75
orifice diameter (mm)	5.42	4.43	3.35
release phase	two-phase	two-phase	two-phase
mass flow (kg/s)	0.431	0.220	0.130
velocity (m/s)	48.95	37.32	38.63
liquid fraction	0.882	0.887	0.887
droplet diameter ( $\mu\text{m}$ )	141.89	239.97	234.17

The side view of the dispersion model result for RS-2F is shown in Figure 20 below. The three concentration values shown are for ERPG-2, ERPG-3, and the estimated visible cloud concentration, respectively. The visible cloud concentration was estimated from dew point calculations using experimental atmospheric and ammonia data.

In the model for RS-2F, the estimated visible cloud concentration of 4800 ppm (based on dewpoint) extends to a maximum distance of 27 m while the visible cloud in Figure 9, shown previously, reaches beyond 80 m. This difference could be due to differences in wind speed and direction, incorrect assumptions in the dew point calculations, or explained by water vapor condensing in the cloud further from the orifice and making the visible cloud appear larger. However, the overall shape of the cloud matches between the model and the video footage. It is worth noting that the PHAST model predicts that the ERPG-2 level extends 150 m away and the

ERPG-3 level extends 44 m away from the orifice, meaning that at ambient temperature, pressurized releases would have a very large impact zone.

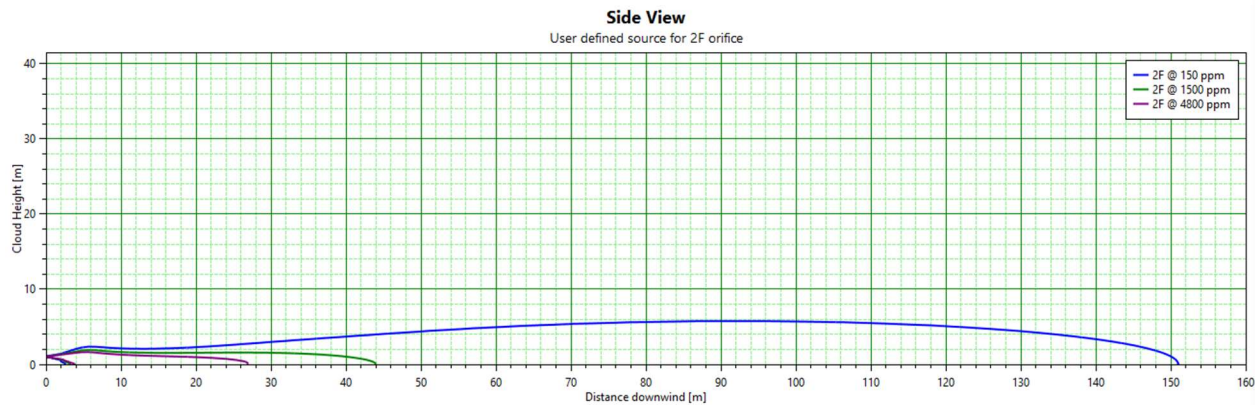


Figure 20: Side view of the PHAST dispersion model for RS-2F for during the release

Figure 21 below shows concentration vs distance plots for the PHAST model predictions and experimental concentration data for RS-2D and RS-2F. Note that experimental data represented by green dots are values where the sensors were maxed out at 1100 ppm. The plots show that the PHAST dispersion models do in fact predict concentrations >1100 ppm in the near field. The far field values are overestimated by PHAST, particularly for RS-2F. However, for both trials at 45 m and 80 m, the predictions are about within a factor of 2 from the experimental results, which is good considering the variance in wind speed, wind direction, and release rate.

A notable feature of the concentration vs distance plots are the dips between 10 and 20 m on the prediction curves. Investigation into the PHAST model revealed this is likely caused by the way PHAST is modeling air entrainment in the expansion zone of the discharge modeling and how the model transitions to the far field dispersion. It is possible that changes to discharge and/or dispersion parameters would smooth out the curves.

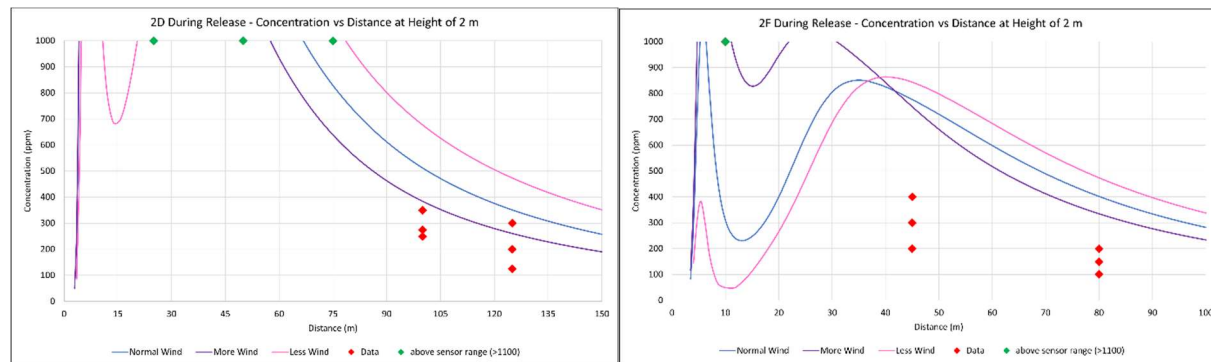
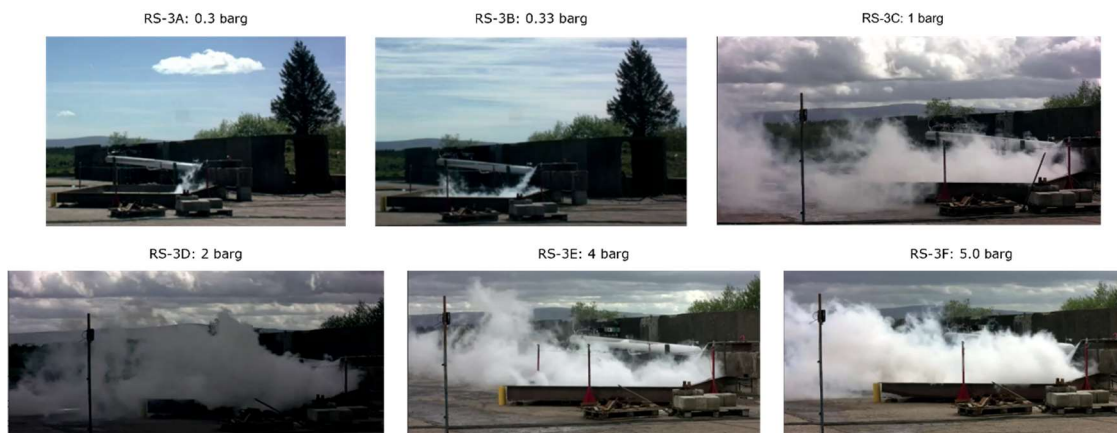


Figure 21: Concentration vs distance experimental data and PHAST model prediction for RS-2D (left) and RS-2F (right) for during the release

### 3.4 Cold Ammonia Release under Nitrogen Pressure (RS-3)

Side view photos of the RS-3 releases of cold/refrigerated ammonia are shown in order of increasing release pressure in Figure 22 below. There seems to be a transition in the visible cloud from 0.33 barg to 1 barg. At lower pressures, the ammonia appears to mostly form a pool with a

small visible cloud due to vapor deflecting off the bund as well as vaporization from the pool. However, at the higher pressures, large visible clouds form and less liquid appeared to form a pool in the bund. However, at the highest pressure of 5 barg, the visible cloud did not appear to extend as far beyond the release point when compared to the 80 m visible clouds seen in multiple RS-2 trials at similar pressures. In both setups, the cold ammonia was pressurized, however, in RS-3 it was in a cold/refrigerated state as well. This indicates that storing and transporting ammonia as a refrigerated pressurized liquid is safer than as an ambient temperature pressurized liquid.



**Figure 22: Illustration of transition from liquid spills to 2-phase flow for cold ammonia releases under pressure**

To further qualitatively analyze where the transition from liquid spills to two-phase releases occurs, the experimental field concentration data was analyzed. The wind speed, release rates, and release pressures for each trial are shown in Table 14. The experimental data for the field concentrations during the release itself and for the first hour post release is shown in Tables 15 and 16, respectively.

Overall, as pressure increases, the release rate increases, and the concentrations measured by the sensors increases. Additionally, compared to the RS-2 trials, the concentrations in the far field during the release are lower. The near field concentrations cannot be compared as the sensors are maxed out in both cases.

As seen visually in Figure 22, the tabulated data seems to show a transition between trials 3B and 3C. For the period during the release, the concentrations increase by about a factor of 2 between the trials. For the period after the release, the same is observed. In contrast, the concentrations do not seem to increase at as high a rate between trials of higher pressure. However, as these releases were angled downward into a bund while RS-2 were done horizontally, there is not enough information to further characterize the transition from liquid spill to two-phase flows.

**Table 14: Weather and release conditions for RS-3 tests for during the release itself**

Variable	RS-3A	RS-3B	RS-3C	RS-3D	RS-3E	RS-3F
wind speed (m/s)	$6.7 \pm 2.2$	$6.8 \pm 2.2$	$13.0 \pm 2.4$	$10.9 \pm 2.7$	$12.5 \pm 2.2$	$13.0 \pm 2.8$
release rate (kg/s)	0.076	0.060	0.40	0.42	0.65	0.93
pressure (barg)	0.3	0.33	1.0	2.0	4.0	5.0

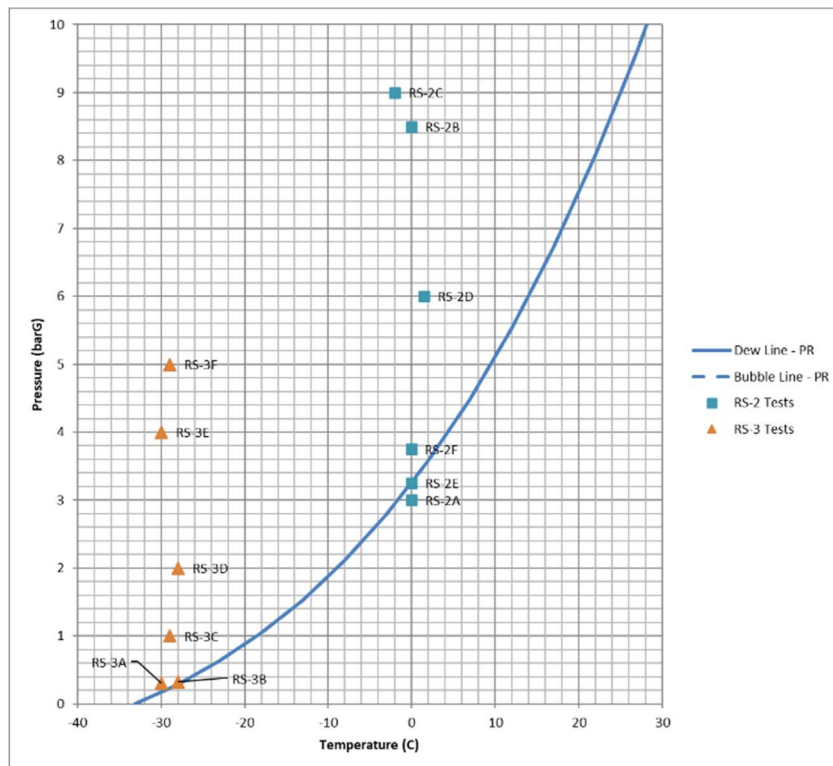
**Table 15: Experimental concentrations (ppm) for RS-3 tests for during the release itself**

Sensor	RS-3A	RS-3B	RS-3C	RS-3D	RS-3E	RS-3F
10 m	>1100	>1100	>1100	>1100	>1100	>1100
45 m	90-130	100-130	175-225	175-225	200-400	300-500
80 m, 2 m	30-45	35-50	70-90	70-100	20-40	60-100
80 m, 10 m	25-35	25-35	60-80	30-110	100-200	150-250

**Table 16: Experimental concentrations (ppm) for RS-3 tests for the 1<sup>st</sup> hour post release**

Sensor	RS-3A	RS-3B	RS-3C	RS-3D	RS-3E	RS-3F
10 m	550-800	400-650	600-900	600-1100	700-1100	700-1100
45 m	60-80	50-80	80-140	50-200	100-300	100-400
80 m, 2 m	25-35	25-35	35-80	15-100	20-40	30-70
80 m, 10 m	10-20	7-15	20-70	20-60	40-140	50-200

The RS-3A and RS-3B tests were conducted with vessel conditions very close to saturation conditions where significant flashing in the release pipework between the vessel and release point possibly leads to smaller liquid fractions in the ejected fluid and resultant reduction in mass flow rate. The level of flashing and resultant liquid fraction in the release to atmosphere is a function of the vessel conditions, the frictional capacity of the release pipe and the geometry of the release. The test conditions RS-2 and RS-3 tests versus the saturation curve for pure ammonia are shown in Figure 23 below.

**Figure 23: Release conditions in each test versus phase diagram (Peng-Robinson)**

As demonstrated in the RS-2 series of tests, for discharge of ambient temperature ammonia liquified under pressure, the liquid released breaks up into fine aerosol because of the superheat energy (typically represented by  $\Delta T = [T_{\text{amb}} - T_{\text{NBP}}]$ ) as has been discussed in previous studies

[12]. No large-scale studies have been done for cold/refrigerated ammonia under pressure for characterizing aerosol formation and potential rainout. The rainout fraction could not be measured in the RS-3 series of tests but were observed qualitatively. It is possible that just the mechanical break-up of liquid into aerosol (versus from the superheat energy present) results in large liquid droplet size and causing some rainout. The two-phase flows observed at high pressures in RS-3 series while deflected of the concrete bund still resulted in some liquid rainout.

## 4 Discussion & Summary

Since the Desert Tortoise and FLADIS tests in 1983 and 1996, respectively, no field testing of anhydrous ammonia releases has been done. After the more recent and successful Jack Rabbit II testing for chlorine releases [3], plans were developed by U.S. Department of Homeland Security for conducting field tests for ammonia releases called Jack Rabbit III (JR-III) [13, 14]. However, there have been significant delays in funding & conduct of the large-scale JR-III tests, which is still needed. In the meantime, a need was recognized by Air Products for getting source term and dispersion data for not just ammonia that is at ambient temperature and compressed at high pressures (7 to 10 barg) as examined previously in Desert Tortoise and FLADIS tests, but also for cold/refrigerated ammonia releases at low to high pressures onto land and water.

Because of decarbonization goals set by different countries, and the demand for blue and green hydrogen in the future, ammonia will be used as a hydrogen carrier [1,2]. Therefore, the demand for ammonia production, use, transport, and handling will increase dramatically in the future. It is important for developing inherently safer designs & practices for storage, transport, and handling of ammonia, which is acutely toxic and can cause irreversible injuries or fatalities upon exposure. Currently, no internationally recognized standards exist for ammonia like they do for facilities and operations handling chlorine, which is also very toxic. It is also important to demonstrate that anhydrous ammonia when handled as a cold/refrigerated liquid (<-30 C temperature; < 1 barg pressure) is inherently safer than storing, transporting, and handling it as an ambient compressed liquid (ambient temperature; 7 to 10 barg pressure).

DNV Spadeadam site, in U.K., was chosen by Air Products for conducting smaller scale field tests, to develop necessary data for a better understanding of the discharge and dispersion of anhydrous ammonia which can cause toxic injuries. Depending on the storage and release conditions, either a two-phase flow (with a dense plume that travels long distances to concentrations of concern) or liquid spills (with buoyant ammonia vapors with limited downwind impact) can result. Spadeadam is a good location for doing such tests. However, because of the unpredictable weather conditions, the RS tests were conducted during appropriate weeks spread over the entire 2022 year. A description has been provided in sections above on the equipment, instrumentation, and data collected.

RS-1 refers to liquid spills (of cold ammonia at very low pressure) into a small 4 m x 4 m concrete bund. A significant amount of cold ammonia was spilled either into a dry concrete bund or into a pond of water in the same bund. The sudden release of cold/refrigerated ammonia into the concrete bund, resulted in a boiling pool that persisted for a while. The visible clouds from the refrigerated releases were isolated to the immediate area around the bund. While the concentrations measured in the immediate vicinity of the bund were high (>1000 ppm limit of the sensors), the measured concentrations 45 m downwind were 300 ppm or less. When refrigerated ammonia was released into a pool of water, more than 50% of the ammonia was absorbed in the water and the remainder behaved like a short duration vapor release, or “puff”.

The downwind concentrations were initially higher for the releases into water than for the releases onto concrete, but the peak concentrations only persisted for a few seconds. As expected, the vaporization rate of ammonia from the aqua ammonia pool was extremely low.

RS-2 refers to releases of ambient ammonia compressed as a liquid at high pressure. The releases were in the horizontal direction out of small 6 mm orifice at different upstream pressures. The fluid discharged for these releases was always in the form of two-phase flow, where the flashed liquid (88% liquid mass vs vapor mass) is always in form of fine aerosol (<250  $\mu\text{m}$ ). There is no liquid separation and rainout observed. As anticipated, based on previous testing at Desert Tortoise and FLADIS experiments and other accidental releases, these pressurized ambient releases resulted in a dense visible cloud and ammonia concentrations exceeding ammonia's ERPG-2 of 150 ppm more than 125 m from the release point for these relatively small (0.1 to 0.5 kg/s) releases under daytime windy conditions. The impact distances would be much larger under low wind speeds and calm (night-time) conditions.

RS-3 refers to releases of cold/refrigerated ammonia from low to high pressure at a 45-degree angle into the small 4 m x 4 m concrete bund. The cold/refrigerated, pressurized ammonia releases were performed to determine the release conditions for which releases could be expected to behave as a pressurized dense aerosol or as a boiling pool. The refrigerated pressurized releases were oriented at the 45-degree downward angle to increase the likelihood of capturing all liquid in the bund area. In hindsight, the variation in release angle made it harder to make definitive characterizations about the transition behavior. It was difficult to accurately estimate the amount of liquid in the bund from the load cells since the ammonia was impinging downward. Dispersion modeling of a downward discharge also was a challenge. Horizontal, refrigerated pressurized releases will be done in the future to further demonstrate the ammonia liquified by refrigeration is inherently safer than ambient ammonia liquified by pressure.

The detailed Red Squirrel test data will be made available to the world scientific & modeling community after completion of the few additional small-scale tests. There is, however, a need for conducting large-scale field tests, like JR III [13, 14], to get needed scientific data to improve the understanding of anhydrous ammonia behavior upon loss of containment particularly in the cold/refrigerated state forming large spills on land and water, in addition to confirming the worst-case impacts when released from ambient pressurized state.

## 5 References

- [1] Tullo, A.H. (2021). Is Ammonia the Fuel of the Future? Industry Sees the Agricultural Chemical as a Convenient Means To Transport Hydrogen, Chemical & Engineering News. <https://cen.acs.org/business/petrochemicals/ammonia-fuel-future/99/i8>
- [2] International Energy Agency. (2022). Ammonia Technology Roadmap. <https://www.iea.org/reports/ammonia-technology-roadmap/executive-summary>
- [3] Nicholson, D, Lian, N., Hedrick, A., Schmidt, E., (2017). Final Test Report for Jack Rabbit (JR) II, ATEC Project No. 2015-DT-DPG-SNIMT-F9735, WDTC-SPD-FTR-001.
- [4] American Industrial Hygienists Association (AIHA), 2020 Emergency Response Planning Guidelines (ERPG) & Workplace Environmental Exposure Levels (WEEL) Handbook.



- [5] U.K. HSE, Assessment of the Dangerous Toxic Load (DTL) for Specified Level of Toxicity (SLOT) and Significant Likelihood of Death (SLOD), <https://www.hse.gov.uk/chemicals/haztox.htm>
- [6] Dharmavaram, S., Pattabathula, V. (2022). The Dakar Ammonia Accident – Analysis of the Worst Ammonia Incident at an Anhydrous Ammonia User. In *Proceedings of the 66<sup>th</sup> Annual Ammonia Safety Symposium*.
- [7] Dharmavaram, S., Pattabathula, V. (2023). Worst Ammonia Accident – Dakar, Senegal; March 1992. *Chemical Engineering Progress*, to be published.
- [8] Goldwire Jr, H. C., McRae, T. G., Johnson, G. W., Hipple, D. L., Koopman, R. P., McClure, J. W., Morris, L.K., & Cederwall, R. T. (1985). *Desert Tortoise series data report: 1983 pressurized ammonia spills* (No. UCID-20562). Lawrence Livermore National Lab., CA (USA).
- [9] Nielsen, M., & Ott, S. (1996). Fladis field experiments. Final report.
- [10] DNV PHAST model (Ver. 8.23), <https://www.dnv.com/software/services/phast/index.html>
- [11] Studer, D.W., Cooper, B.A., & Doelp, L.C. (1988). Vaporization and dispersion modeling of contained refrigerated liquid spills. *Plant/Operations Progress*, Vol. 7 (2), pp 127-135.
- [12] Johnson, D.W. Woodward J.L.. (1999). *RELEASE - A Model with Data to Predict Aerosol Rainout in Accidental Releases*. Center for Chemical Process Safety/AIChE (CCPS).
- [13] Fox, S., Meris, R., & McMasters, S. (2022). Jack Rabbit III: Filling Critical Atmospheric Dispersion Modeling Gaps for Emergency Planning and Response, *Twenty-sixth Annual George Mason University Conference on Atmospheric Transport and Dispersion Modeling*
- [14] U.S. Department of Homeland Security, Chemical Security Analysis Center, Science and Technology Directorate. (2021) Jack Rabbit III Initiatives. <https://www.cisa.gov/sites/default/files/publications/2020-seminars-jack-rabbit-III-508.pdf>